Original Research

Mycobacterium avium paratuberculosis infection augments innate immune responses following intestinal epithelial injury

Charles Johnson[1], Michael Wannemuehler[2] and Jesse Hostetter[1]

[1]Department of Veterinary Pathology, College of Veterinary Medicine, Iowa State University, Ames, IA 50011-1250, USA; [2]Department of Veterinary Microbiology and Preventative Medicine, College of Veterinary Medicine, Iowa State University, Ames, IA 50011-1250, USA
Corresponding author: Jesse Hostetter. Email: jesseh@iastate.edu

Abstract

We wanted to determine if augmented innate immune activation is associated with lesion development in a mycobacterial enhanced intestinal injury model. We evaluated the local immune response in a *Mycobacterium avium paratuberculosis* + dextran sulfate sodium (*Map* + DSS) model using BALB/c and severe combined immunodeficient (SCID) mice. *Map* + DSS BALB/c and SCID mice displayed a similar disease phenotype. Moreover, *Map* + DSS SCID mice had increased expression of interleukin 1β (IL-1β), tumor necrosis factor α (TNF-α), inducible nitric oxide synthase (iNOS) and increased numbers of F4/80 positive cells. Additionally, *Map* antigen is co-localized with iNOS and IL-1β positive cells. This suggests that subclinical *Map* infection promotes innate immune activation following injury to the intestinal epithelium.

Keywords: Dextran sulfate sodium, innate cytokines, *Mycobacterium avium paratuberculosis*, subclinical infection, enhanced intestinal inflammation

***Experimental Biology and Medicine* 2014; 239: 436–441. DOI: 10.1177/1535370213518280**

Introduction

The pathogenesis of inflammatory bowel disease (IBD) is complex with host genetics, microbiota, and environmental stimuli all likely contributing to the onset of clinical disease.[1] It is probable that multiple factors act in concert to promote progressive inflammation rather than a single event resulting in the disease phenotype. For example, subclinical intestinal cytomegalovirus infection, a pathogen known to infect macrophages, exacerbates subsequent dextran sulfate sodium (DSS)-mediated intestinal inflammation.[2,3] This finding suggests that enteric pathogens, in particular, intracellular pathogens, may influence the progression of IBD. However, the mechanisms for how this occurs are not understood.

Mycobacterium avium paratuberculosis (*Map*) has a tropism for macrophages and historically has been incriminated as having a role in Crohn's disease (CD), but the role, if any, of *Map* in CD is controversial.[4] However, recent studies have suggested that *Map* may act as an immune modulator in susceptible individuals thereby exacerbating mucosal inflammation initiated by other causes.[5] In support of this hypothesis, oral exposure to *Map*, without intestinal colonization, is capable of augmenting intestinal inflammation in interleukin 10 (IL-10) deficient mice.[6]

Excessive activation of the innate immune system is thought to play an important role in the pathogenesis of IBD. For example, IL-1β appears to have an important role, as evidenced by enhanced secretion of IL-1β by mononuclear cells isolated from the inflamed mucosa of patients with CD.[7] However, it is not clear how an infection with an opportunistic pathogen, such as *Map*, that targets macrophages and are an significant source of IL-1β would impact mucosal macrophage function especially in situations where there is an underlying genetic defect that compromises innate immune regulation such as polymorphisms in NOD2.[8]

We have previously reported that *Map* infection of BALB/c mice did not induce detectable disease or intestinal inflammation. However, when *Map* infected mice were given a low dose (2%) of DSS, which alone was insufficient to cause significant clinical disease, severe intestinal ulceration, and hemorrhage occurred. This correlated with marked weight loss and rectal bleeding.[9] Since *Map* is a pathogen of macrophages we hypothesized that enhanced innate immune activation contributes to lesion development. To test our hypothesis, we utilized BALB/c and severe combined immunodeficient (SCID) mice.

Materials and methods

Animals

BALB/c and SCID/C.B-17 6–8 week-old male mice weighing approximately 22–24 g were housed in

micro-isolation units. All animal experiments were approved by the Institutional Animal Care and Use Committee of Iowa State University.

Bacterial inoculum

The *Map* strain K10 was a field isolate obtained from the National Animal Disease Center (Ames, IA) and maintained at 37°C in Middlebrook 7H9 broth supplemented with mycobactin J. Logarithmic growth-phase bacteria were resuspended in sterile saline n and adjusted to a final concentration of 1×10^9 colony-forming units/mL. Controls were given a sham inoculation of saline. The *Map* inoculum was shown to have greater than 90% viability via fluorescein diacetate staining and flow cytometry. In addition, challenge inocula were confirmed negative for contaminants by streaking onto sheep blood agar plates.

Experimental design

Three separate experiments were conducted with 10–11 BALB/c mice per treatment group; two separate experiments were performed with SCID mice with 4–5 mice per treatment group. In all experiments, mice were assigned to one of two groups and either given a single intraperitoneal sham injection of saline or *Map*. Following inoculation, body weights of the mice were measured at weekly intervals. At 90 days post-infection, acute intestinal injury was chemically induced by administering a suboptimal concentration of 2% DSS (MP Biomedicals, Solon, OH) in the drinking water for six days to a subset of infected and uninfected mice. While the mice were administered DSS, they were weighed daily and on day 6 all of the mice were euthanized with CO_2. At necropsy, body weights, colon, and cecal length were measured.

Histopathology

At necropsy, samples of liver, spleen, small and large intestine, and mesenteric lymph node were fixed in 10% neutral buffered formalin, processed by routine methods and stained with hematoxylin and eosin. Cecal histologic lesion scores were generated using a scoring system previously described.[9]

Immunohistochemistry

For immunohistochemistry (IHC), antigen retrieval was accomplished by incubating slides with 0.1% triton X-100 in PBS for IL-1β; microwaving in citrate buffer pH 6 for tumor necrosis factor α (TNF-α) and arginase; microwaving in a pH 10 citrate buffer for inducible nitric oxide synthase (iNOS); and covering slides with 2% protease for F4/80. Slides were then blocked with 10% normal goat serum. The primary antibodies were used at the following dilutions: IL-1β at 1:500 and TNF-α at 1:2000 (Santa Cruz Biotechnology, Inc; Santa Cruz, CA), iNOS at 1:1500 (Upstate, Billerica, MA), arginase at 1:6000 (Fitzgerald Industries; Concord, MA), and F4/80 at 1:1000 (eBioscience, San Diego, CA). All antibodies were incubated overnight at 4°C. Biotinylated goat anti-rabbit IgG or goat anti-rat IgG $F(ab')_2$ fragment (for F4/80) secondary antibodies were used. Horseradish peroxidase (HRP)-streptavidin was then added to the slides followed by 3,3′-diaminobenzidine (DAB). A subset of slides was then stained for *Map* antigen using a polyclonal rabbit anti-*M. bovis* antibody that has extensive cross-reactivity with *Map*.[10] Rabbit anti-*M. bovis* (Dako Cytomation, Carpinteria, CA) was added at 1:4000. Alkaline phosphatase–streptavidin was added to the slides followed by Vector Red Substrate. For IHC evaluation, only epithelium and cells in the lamina propria were scored. The following scoring system was used: 0 – no immunoreactivity, 1 – occasional dim immunoreactivity within isolated cells, 2 – multifocal intense immunoreactivity within small clusters of cells (<10 cells), 3 – frequent intense immunoreactivity within large cell clusters (>20 cells), 4 – nearly diffuse intense immunoreactivity of cells.

Statistical analysis

Changes in body weight were analyzed using an analysis of variance (ANOVA) model with repeated measures. *Map* infection or saline inoculation, DSS or water administration, day and their interactions were considered as fixed effects, with animal being the subject of repeated measures. On each day, the treatment group means were compared first with an overall *F* test and then followed by *post hoc* Tukey–Kramer's *t* test for multiple comparisons if the *F* test was significant. A *P* value of <0.05 was considered significant. For all other parameters, treatment group means were compared first with an overall *F* test and then followed by *post hoc* Student's *t* test with group mean differences considered significant if the *P* value was <0.05. Data are presented as the mean value ± standard error of the mean except where stated otherwise.

Results

We hypothesized that underlying *Map* infection augments innate immune responses during mucosal injury. Infection was confirmed by the isolation of *Map* from multiple tissues of SCID and BALB/c mice, including the cecum/large intestine (data not shown). We evaluated the development of clinical disease (weight loss) and inflammation (histopathology) in the cecum in these two mouse strains.

We found that weight loss was similar between SCID and BALB/c mice. Inoculation with *Map* alone did not induce weight loss prior to DSS administration (see Table 1 for data). However, DSS treatment of *Map* infected BALB/c and SCID mice resulted in significant weight loss (Table 1, $P < 0.05$) which was most pronounced on day 6 of DSS administration. DSS alone caused modest but significant weight loss in the SCID mice; however, this was significantly less than the combination of *Map* + DSS in this group (Table 1, $P < 0.05$).

The histopathologic appearance of the cecum was similar between *Map* infected BALB/c and SCID mice given DSS (Figure 1). *Map* infection alone did not induce significant intestinal microscopic lesions in SCID or BALB/c. DSS treatment of *Map* infected SCID and BALB/c mice yielded the most severe intestinal lesions consisting of mucosal ulceration, hemorrhage, and neutrophil

Table 1 Changes in body weight (g) during DSS treatment

	0	1	2	3	4	5	6
Control							
BALB/c	0	0.04 ± 0.20	−0.08 ± 0.23	−0.02 ± 0.26	0.01 ± 0.23	−0.08 ± 0.29	−0.04 ± 0.34
SCID	0	0.15 ± 0.28	0.38 ± 0.18	0.48 ± 0.06	0.40 ± 0.20	0.45 ± 0.10	0.43 ± 0.17
DSS only							
BALB/c	0	0.12 ± 0.09	−0.05 ± 0.10	−0.15 ± 0.12	−0.4 ± 0.16	−0.20 ± 0.18	−0.48 ± 0.20
SCID	0	0.13 ± 0.18	0.00 ± 0.18	0.10 ± 0.24	0.18 ± 0.42	−0.68 ± 0.23*	−0.33 ± 0.18*
Map only							
BALB/c	0	0.08 ± 0.11	0.24 ± 0.06	0.31 ± 0.11	0.83 ± 0.64	0.31 ± 0.25	0.3 ± 0.27
SCID	0	0.38 ± 0.59	0.55 ± 0.45	0.33 ± 0.46	0.53 ± 0.27	0.35 ± 0.22	0.68 ± 0.37
Map + DSS							
BALB/c	0	0.19 ± 0.11	0.08 ± 0.11	−0.06 ± 0.12	−0.11 ± 0.21	−0.61 ± 0.24	−1.95 ± 0.50*
SCID	0	0.52 ± 0.40	0.78 ± 0.37	0.42 ± 0.33	0.25 ± 0.27	−0.65 ± 0.27*	−1.57 ± 0.27**

**SCID Map + DSS (with p-value <0.05) is different from all of the other DSS treatment groups. *SCID DSS is only different than the control (p-value <0.05) at day 6 of DSS. DSS: dextran sulfate sodium; *Map*: *Mycobacterium avium paratuberculosis*; SCID: severe combined immunodeficient.

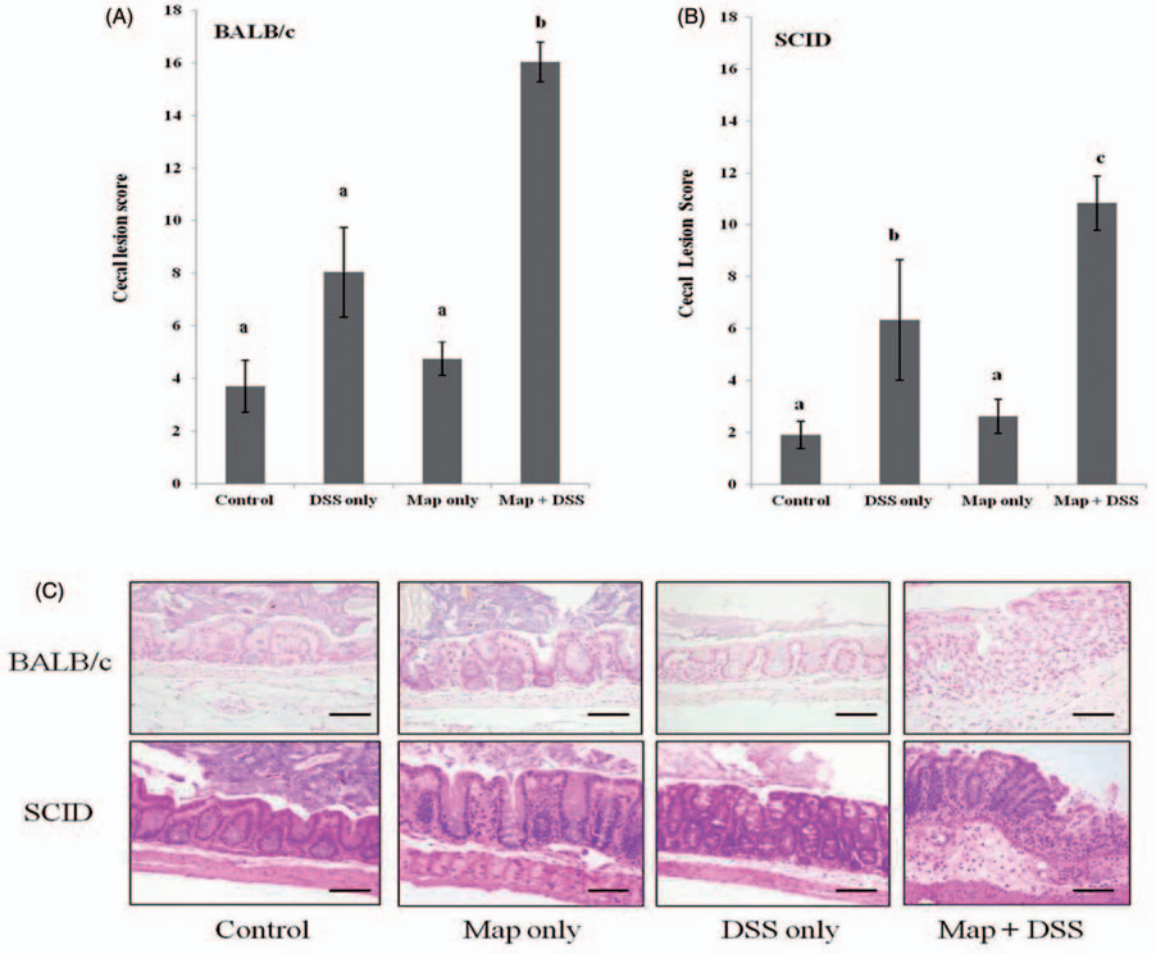

Figure 1 Cecal histologic lesion scores for BALB/c (A) and SCID (B) mice inoculated with saline (control); infected with *Map* only (*Map* only); inoculated with saline and treated with DSS (DSS only); and mice infected with *Map* and treated with DSS (*Map* + DSS). Means with different letters above the bars are significantly different ($P < 0.05$). Data are represented as the mean ± standard error of the means from three separate experiments for the BALB/c mice, including 22 DSS only mice, 25 *Map* + DSS mice, eight *Map*-only mice and nine control mice. For the SCID mice, the data represent the mean ± standard error of the means from two separate experiments including six *Map* + DSS mice, four *Map* only, four DSS only mice, and four control mice. Representative photomicrographs (C) of ceca from control, *Map* only, DSS only, and *Map* + DSS BALB/c and SCID mice. Note the mucosal ulceration, submucosal edema, and compensatory hyperplasia of the adjacent cecal glandular epithelium in the *Map* + DSS SCID mouse. There is moderate glandular epithelial hyperplasia in the cecal mucosa of the DSS only SCID mouse. There is mucosal ulceration with collapse and condensation of the remnant stroma in the *Map* + DSS BALB/c mouse. Lesions were not identified in the *Map* only and control BALB/c or SCID mice. H&E; bar = 50 μm. DSS: dextran sulfate sodium; H&E: Hematoxylin and eosin; *Map*: *Mycobacterium avium paratuberculosis*; SCID: severe combined immunodeficient

infiltration. In SCID mice, DSS treatment of uninfected mice resulted in a modest increase in cecal inflammation characterized by mild gland proliferation and rare epithelial ulceration; however this did not reach the severity of the *Map* + DSS group. When histologic lesions were scored, *Map* + DSS BALB/c and SCID mice had the highest lesion scores (Figure 1, $P < 0.05$).

The similarities in the pattern of clinical disease and intestinal pathology between *Map* infected BALB/c and SCID mice given DSS supported our hypothesis that *Map* enhancement of intestinal injury is driven by innate immune responses. In particular, this suggested that macrophages are a critical cell type in our model since *Map* is a pathogen of macrophages.[11] We have previously demonstrated that cecal F4/80 positive cells, a marker for macrophages, co-localize with acid-fast bacilli in the cecum.[9] To further define the role of macrophages in our model we next wanted to assess the relative number of macrophages within the ceca of SCID mice. *Map* + DSS mice had a greater number of F4/80 positive cells relative to all other treatment groups (Figure 2D). Additionally, DSS only mice had greater numbers of F4/80 positive cells compared to control and *Map* only mice ($P < 0.0009$).

We next sought to evaluate the activation status of intestinal macrophages in our model by performing IHC for arginase, a marker of wound-healing and alternatively activated macrophages, and iNOS, a marker associated with classically activated macrophages.[12,13]

Positive iNOS immunoreactivity in DSS only mice was confined to the cytoplasm of apical enterocytes associated

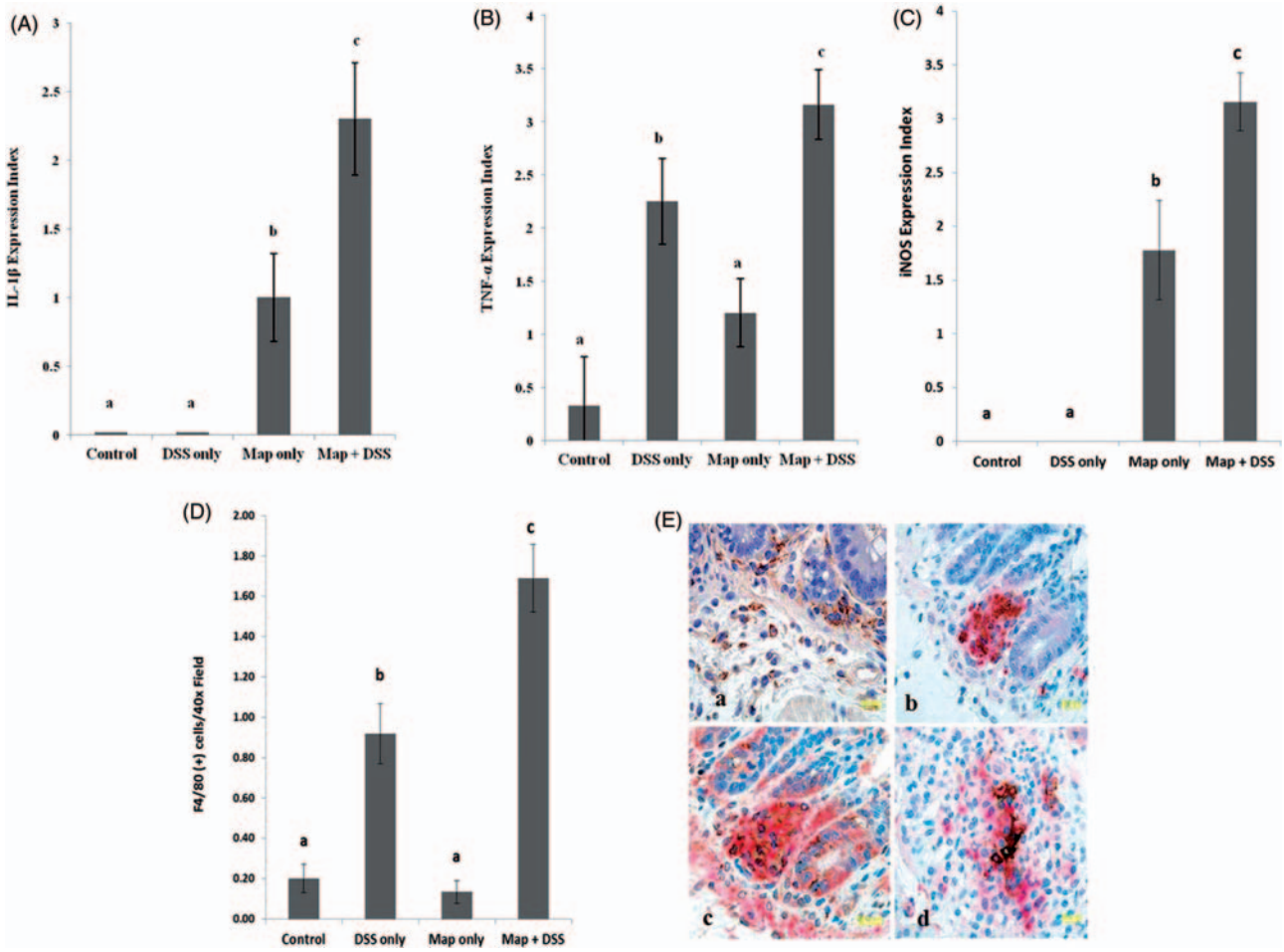

Figure 2 IL-1β (A), TNF-α (B), and iNOS (C) expression index scores in the ceca from SCID mice inoculated with saline (control); infected with *Map* only (*Map* only); inoculated with saline and treated with DSS (DSS only); and mice infected with *Map* and treated with DSS (*Map* + DSS). Means with different letters above the bars are significantly different ($P < 0.05$). Data are represented as the mean ± standard error of the means from two separate experiments including six *Map* + DSS mice, four *Map* only, four DSS only mice, and three control mice for IL-1β and TNF-α. For iNOS, data are represented as the mean ± standard error of the means from two separate experiments including three *Map* + DSS mice, three *Map* only, three DSS only mice, and three control mice. (D) Average number of F4/80 + cells per 40x field in the ceca from mice inoculated with saline (control); infected with *Map* only (*Map* only); inoculated with saline and treated with DSS (DSS only); and mice infected with *Map* and treated with DSS (*Map* + DSS). Means with different letters above the bars are significantly different ($P < 0.05$). Data are represented as the mean ± standard error of the means from two separate experiments including 4 *Map* + DSS mice, 3 *Map* only, 3 DSS only mice, and 3 control mice. Representative photomicrographs (E) from SCID mice infected with *Map* and treated with DSS demonstrating F4/80 (a), *Map* and pro-IL-1β (b), *Map* and arginase (c), and *Map* and iNOS immunoreactivity (d) in the ceca. F4/80 immunoreactivity was primarily confined to the submucosa and cecal crypts. Immunoreactivity for *Map* was present within the cytoplasm of cells with macrophage type morphology. F4/80, pro-IL-1β, arginase, and iNOS stains are brown, whereas the *Map* stain is red. Bar = 50 μm. DSS: dextran sulfate sodium; IL-1β: interleukin 1β; iNOS: inducible nitric oxide synthase; *Map*: *Mycobacterium avium paratuberculosis*; SCID: severe combined immunodeficient; TNF-α: tumor necrosis factor α

with areas of mucosal ulceration and erosion. For *Map* infected mice cytoplasmic iNOS positive staining was confined to foci of granulomatous inflammation subsequently confirmed to contain *Map* antigen. iNOS immunoreactivity was not observed in control mice. *Map* + DSS infected mice had a higher iNOS score relative to all other treatment groups (Figure 2C) while *Map* only infected mice had higher iNOS immunoreactivity scores compared to DSS only and control mice.

There was diffuse cytoplasmic arginase immunoreactivity throughout the lamina propria of the intestinal mucosa in mice of all treatment groups. There was a trend for decreased arginase immunoreactivity in DSS only mice but this did not reach statistical significance (data not shown).

Because macrophages are a significant source of innate cytokines we next wanted to assess the expression of IL-1β and TNF-α in the cecal mucosa of SCID mice. The most frequent and intense immunoreactivity for both IL-1β and TNF-α was in the *Map* + DSS group (Figure 2A and B). IL-1β and TNF-α expression were strongest in the lamina propria. A low frequency and intensity of cells staining positive for IL-1β and TNF-α was observed in mice infected with *Map* only. IL-1β protein was not detected in control mice or in uninfected mice given DSS. TNF-α was expressed in the lamina propria of uninfected mice given DSS, but this did not reach the level of infected mice given DSS. Lastly, we wanted to know if *Map* antigen co-localized with a subset of these activation and pro-inflammatory markers so dual IHC for iNOS, arginase, IL-1β and *Map* antigen was performed. *Map* antigen co-localized with all of these markers, but not all *Map* antigen positive cells were dual positive (Figure 2E).

Discussion

Dysregulation of innate immune responses has been shown to be an early component in the development of progressive intestinal inflammation.[14] Therefore, it is imperative for the host to recognize danger signals associated with penetrating microbial agents, including components of the microbiota, and eliminate them without generating excessive inflammation and mucosal injury. We hypothesized that certain enteric pathogens disrupt homeostatic mechanisms to favor inflammation. For example, superinfections of IBD patients with enteric pathogens such as *Campylobacter jejuni* can lead to an acute relapse of disease.[15] Furthermore, this may be especially valid in situations where there is an underlying genetic defect that compromises innate immune regulation such as polymorphisms in NOD2.[8] In this study, we induced chronic subclinical infection with an enteric pathogen, *Map*. Chronic infection by itself did not induce significant clinical disease, mucosal pathology, or alterations in macrophage number or activation status within the cecal mucosa. However, after a mild mucosal injury in infected mice, there was enhanced innate immune activation and increased numbers of mucosal macrophages. This correlated with significant microscopic inflammation and onset of clinical disease.

In *Map* + DSS mice that lack adaptive immune responses we saw similar clinical disease and mucosal pathology as the immunocompetent BALB/c mice suggesting that innate immune mechanisms play a central role in *Map* enhanced disease. Our immunohistochemical data supports this hypothesis. *Map* + DSS treated SCID mice had increased numbers of mucosal macrophages with a shift towards a classically activated phenotype as indicated by increased iNOS, IL-1β, and TNF-α expression. *Map* antigen co-localized with several of these markers, but not all *Map* antigen positive cells were dual labeled suggesting exposure to an additional stimulus, such as the luminal microflora, may be required for full activation. Increased expression of TNF-α and IL-1β was not unexpected considering both cytokines are increased in mouse models of IBD in which DSS is administered.[16]

In summary, our data suggest that a persistent enteric pathogen, such as *Map*, is capable of augmenting the innate immune response during acute intestinal injury, as evidenced by increased expression of IL-1β and TNF-α in *Map* + DSS mice. We propose that *Map* infection lowers the activation threshold of mucosal macrophages. Further inflammatory triggers, such as exposure to the luminal microflora following an epithelial insult, allow for increased IL-1β and TNF-α production by macrophages, which promotes overt cecal inflammation and clinical disease. Future studies should examine whether our findings are specific to *Map* by exposing mice to other pathogen capable of establishing occult intestinal infections such as *M. avium* subsp. *avium*. Furthermore, future studies with neutralizing antibodies against IL-1β and TNF-α would be necessary to establish that the enhanced disease in our model is driven by innate cytokines.

Author contributions: All authors participated in the design, interpretation of results and analysis of the data. Each of the authors participated in the preparation of the manuscript; however, JMH and CSJ were primarily responsible for the initial drafts of the manuscript. JMH was responsible for the overall conduct of the project and experimental design. CSJ conducted the majority of the *in vivo* and *ex vivo* experiments. MJW provided significant input in experimental design, the murine model and manuscript preparation.

ACKNOWLEDGEMENTS

We thank Elise Huffman and Dr Brandon Plattner for technical assistance and Dr Chong Wang for help with statistical analysis. This work was funded through an Iowa State University research grant and the Iowa Healthy Livestock Initiative.

REFERENCES

1. Mayer L. Evolving paradigms in the pathogenesis of IBD. *J Gastroenterol* 2010;**45**:9–16
2. Redman TK, Britt WJ, Wilcox CM, Graham MF, Smith PD. Human cytomegalovirus enhances chemokine production by lipopolysaccharide-stimulated lamina propria macrophages. *J Infect Dis* 2002;**185**:584–90
3. Onyeagocha C, Hossain MS, Kumar A, Jones RM, Roback J, Gewirtz AT. Latent cytomegalovirus infection exacerbates experimental colitis. *Am J Pathol* 2009;**175**:2034–42

4. Mendoza JL, Lana R, Diaz-Rubio M. *Mycobacterium avium* subspecies *paratuberculosis* and its relationship with Crohn's disease. *World J Gastroenterol* 2009;**15**:417–22
5. Sibartie S, Scully P, Keohane J, O'Neill S, O'Mahony J, O'Hanlon D, Kirwan WO, O'Mahony L, Shanahan F. *Mycobacterium avium* subsp. *paratuberculosis* (MAP) as a modifying factor in Crohn's disease. *Inflamm Bowel Dis* 2010;**16**:296–304
6. Singh UP, Singh S, Singh R, Karls RK, Quinn FD, Potter ME, Lillard JW Jr. Influence of *Mycobacterium avium* subsp *paratuberculosis* on colitis development and specific immune responses during disease. *Infect Immun* 2007;**75**:3722–8
7. Mahida YR, Wu K, Jewell DP. Enhanced production of interleukin 1-beta by mononuclear cells isolated from mucosa with active ulcerative colitis of Crohn's disease. *Gut* 1989;**30**:835–8
8. Ogura Y, Bonen DK, Inohara N, Nicolae DL, Chen FF, Ramos R, Britton H, Moran T, Karaliuskas R, Duerr RH, Achkar JP, Brant SR, Bayless TM, Kirschner BS, Hanauer SB, Nuñez G, Cho JH. A frameshift mutation in NOD2 associated with susceptibility to Crohn's disease. *Nature* 2001;**411**:603–6
9. Johnson CS, Wannemuehler MJ, Hostetter JM. Persistent enteric mycobacterial infection enhances sensitivity to acute mucosal injury. *Exp Biol Med* 2011;**236**:36–43
10. Brees DJ, Reimer SB, Cheville NF, Florance A, Thoen CO. Immunohistochemical detection of *Mycobacterium paratuberculosis* in formalin-fixed, paraffin-embedded bovine tissue sections. *J Vet Diagn Invest* 2000;**12**:60–63
11. Weiss DJ, Souza CD. Review paper: modulation of mononuclear phagocyte function by *Mycobacterium avium* subsp. *paratuberculosis*. *Vet Pathol* 2008;**45**:829–41
12. Shearer JD, Richards JR, Mills CD, Caldwell MD. Differential regulation of macrophage arginine metabolism: a proposed role in wound healing. *Am J Physiol* 1997;**272**:E181–190
13. MacMicking J, Xie QW, Nathan C. Nitric oxide and macrophage function. *Annu Rev Immunol* 1997;**15**:323–50
14. Blumberg RS. Inflammation in the intestinal tract: pathogenesis and treatment. *Dig Dis* 2009;**27**:455–64
15. Stallmach A, Carstens O. Role of infections in the manifestation or reactivation of inflammatory bowel diseases. *Inflamm Bowel Dis* 2002;**8**:213–8
16. Egger B, Bajaj-Elliott M, MacDonald TT, Inglin R, Eysselein VE, Buchler MW. Characterisation of acute murine dextran sodium sulphate colitis: cytokine profile and dose dependency. *Digestion* 2000;**62**:240–48

(Received September 5, 2013, Accepted October 30, 2013)